AD-A150 987 CURRENT DISTRIBUTION IN A PLASMA EROSION OPENING SWITCH 1/1
(U) NAVAL RESEARCH LAB WASHINGTON DC B V WEBER ET AL.
27 FEB 85 NRL-MR-5515

UNCLASSIFIED F/G 20/9 NL

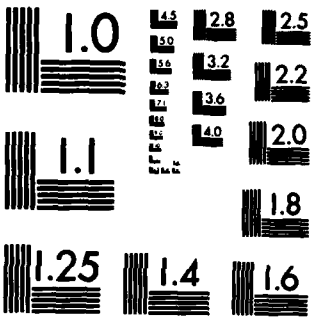

MICROCOPY RESOLUTION TEST CHART
NATIONAL BUREAU OF STANDARDS-1963-A

NRL Memorandum Report 5515

Current Distribution in a Plasma Erosion Opening Switch

B. V. WEBER,* R. J. COMMISSO, R. A. MEGER, J. M. NERI,
W. F. OLIPHANT, AND P. F. OTTINGER*

Plasma Technology Branch
Plasma Physics Division

**JAYCOR, Inc.*
Alexandria, VA 22304

February 27, 1985

This work was supported by the Defense Nuclear Agency under Subtask T99QAXLA, work units 00038 and 00023, work unit title "Advanced Simulation Concepts," the Department of Energy and the Office of Naval Research.

NAVAL RESEARCH LABORATORY
Washington, D.C.

SECURITY CLASSIFICATION OF THIS PAGE

REPORT DOCUMENTATION PAGE

1a REPORT SECURITY CLASSIFICATION UNCLASSIFIED	1b. RESTRICTIVE MARKINGS
2a SECURITY CLASSIFICATION AUTHORITY	3 DISTRIBUTION / AVAILABILITY OF REPORT Approved for public release; distribution unlimited.
2b DECLASSIFICATION / DOWNGRADING SCHEDULE	
4 PERFORMING ORGANIZATION REPORT NUMBER(S) NRL Memorandum Report 5515	5. MONITORING ORGANIZATION REPORT NUMBER(S)
6a. NAME OF PERFORMING ORGANIZATION Naval Research Laboratory 6b OFFICE SYMBOL (If applicable) Code 4770	7a. NAME OF MONITORING ORGANIZATION
6c. ADDRESS (City, State, and ZIP Code) Washington, DC 20375-5000	7b. ADDRESS (City, State, and ZIP Code)
8a. NAME OF FUNDING / SPONSORING ORGANIZATION DNA and DOE 8b. OFFICE SYMBOL (If applicable)	9. PROCUREMENT INSTRUMENT IDENTIFICATION NUMBER
8c. ADDRESS (City, State, and ZIP Code) Washington, DC 20305 Washington, DC 20545	10. SOURCE OF FUNDING NUMBERS PROGRAM ELEMENT NO. 62715H; PROJECT NO.; TASK NO. DE-AI 08-79DP 40092; WORK UNIT ACCESSION NO. DN320-094

11 TITLE (Include Security Classification)

Current Distribution in a Plasma Erosion Opening Switch

12. PERSONAL AUTHOR(S)

Weber, B.V.,* Commisso, R.J., Meger, R.A., Neri, J.M., Oliphant, W.F., and Ottinger, P.F.*

13a. TYPE OF REPORT	13b. TIME COVERED	14. DATE OF REPORT (Year, Month, Day)	15. PAGE COUNT
Interim	FROM 1/83 TO 12/83	1985 February 27	18

16 SUPPLEMENTARY NOTATION

*JAYCOR, Inc., Alexandria, VA 22304 (Continues)

17 COSATI CODES			18. SUBJECT TERMS (Continue on reverse if necessary and identify by block number)
FIELD	GROUP	SUB-GROUP	Plasma erosion opening switch; Anomalous resistivity; Inductive storage

19 ABSTRACT (Continue on reverse if necessary and identify by block number)

The current distribution in a plasma erosion opening switch is determined from magnetic field probe data. During the closed state of the switch the current channel broadens rapidly. The width of the current channel is consistent with a bipolar current density limit imposed by the ion flux to the cathode. The effective resistivity of the current channel is anomalously large. Current is diverted to the load when a gap opens near the cathode side of the switch. The observed gap opening can be explained by erosion of the plasma. Magnetic pressure is insufficient to open the gap.

Add [illegible] Circuit Computations

20 DISTRIBUTION / AVAILABILITY OF ABSTRACT ☒ UNCLASSIFIED/UNLIMITED ☐ SAME AS RPT ☐ OTIC USERS	21. ABSTRACT SECURITY CLASSIFICATION UNCLASSIFIED
22a NAME OF RESPONSIBLE INDIVIDUAL B. V. Weber	22b. TELEPHONE (Include Area Code) (202) 767-2298; 22c. OFFICE SYMBOL Code 4770

DD FORM 1473, 84 MAR 83 APR edition may be used until exhausted.
All other editions are obsolete.

SECURITY CLASSIFICATION OF THIS PAGE

16. SUPPLEMENTARY NOTATION (Continued)

This work was supported by the Defense Nuclear Agency under Subtask T99QAXLA, work units 00038 and 00023, work unit title "Advanced Simulation Concepts," the Department of Energy and the Office of Naval Research.

CURRENT DISTRIBUTION IN A PLASMA EROSION OPENING SWITCH

The Plasma Erosion Opening Switch (PEOS) consists of a low density ($\sim 10^{13}$ cm^{-3}) plasma injected across a vacuum feed line in a pulsed power generator. The PEOS can conduct high current ($\sim$ MA), open quickly (<10 ns), and withstand high voltage ($\sim$ MV). This switching technique has been used in inductive energy storage experiments demonstrating pulse compression, voltage multiplication and power multiplication.[1] The PEOS is used routinely at several laboratories for other types of power conditioning including prepulse suppression,[2] pulse sharpening[3] and multimodule jitter reduction.[4] In this letter the current flow pattern in a PEOS plasma is determined from magnetic field probe measurements. The current channel in the PEOS plasma broadens as the current through the switch increases. The current channel is wide, $>>c/\omega_{pe}$, inferring an anomalously high resistivity. The measured current channel width is consistent with a theoretical model that predicts a current density limit imposed by the ion flux to the cathode. Switching occurs when a gap is formed between the plasma and the cathode.

The Gamble I generator[5] at the Naval Research Laboratory is configured with a PEOS system and a short circuit load as shown in Fig. 1. Three plasma guns[6] inject a carbon plasma into the region between the screen and the cylindrical center conductor. The generator is fired about 1.5 μs later, applying a negative high voltage pulse (-1 MV, 50 ns FWHM) to the center conductor. Currents on the generator (I_G) and load (I_L) sides of the switch are plotted in Fig. 2. The current through the 180 nH storage inductance and PEOS plasma increases to 150 kA in 40 ns, while I_L remains small. During the next 10 ns, I_L increases to 200 kA and the switch current (I_G-I_L) becomes small, indicating the switch is open.

Manuscript approved November 20, 1984.

Five small probes are used to measure the local magnetic field in the PEOS during fast opening shots. The probes are potted inside 5 mm diameter quartz tubes and inserted into the switching region through the screen. The azimuthal field, $B_\theta(t)$, is measured at the locations shown in Fig. 1. Five axial (z) locations are sampled on a single shot, at the same radial (r) location. The probes are moved to different radial locations to scan the cross section. The probes are calibrated relative to the Rogowski loops that measure I_L and I_G, using data from shots with no plasma injection. In this case, $I = I_G = I_L$ and

$$I\ (kA) = 5r(cm)\ B_\theta(kG). \qquad (1)$$

Eq. (1) holds if B_θ is azimuthally symmetric, and gives the total current through a circle of radius r. Measurements of $B_\theta(\theta)$ during fast opening shots indicate that B_θ is reasonably symmetric (±5%) so that Eq. (1) can be used to approximate the current distribution in the plasma.

Probe data, B_θx5r(kA), are plotted as a function of time in Fig. 3 for r = 3, 4 and 5 cm. The corresponding load currents are shown in Fig. 2. The uncertainty in the measurements due to digitizing, calibration, probe orientation and timing is estimated to be ± 20 kA. Experimentally, the probes do not perturb the plasma. The presence of the probes does not affect the measured currents I_G and I_L, and the signal obtained from a given probe is independent of the location of other probes.

The data in Fig. 3 are used to map out current streamlines in the PEOS plasma before, during and after opening. Two times before opening are marked by arrows in Fig. 2 at t = 16 and 36 ns. These times correspond to the first nonzero points of the r = 5 cm probe signals at z = 4 and 6 cm which identify the downstream edge of the current channel. The width of the current channel is determined by comparing adjacent probe signals. For example, at

t = 36 ns the downstream edge of the current channel is at r = 5 cm, z = 6 cm. The 130 kA generator current is divided between z = 2 and 6 cm with 100 kA between z = 4 and 6 cm. The probe data in the rest of the r-z cross section determine the current channel between the outer and inner conductors, shown in Fig. 4. Data taken at I_L = 100 and 200 kA, shown by arrows in Fig. 2, determine the current streamlines during and after opening. Dashed lines in Fig. 4 show possible streamlines outside the data grid, consistent with the measured current I_L.

Figs. 4(a) and (b) show that current is conducted radially from the outer conductor to the inner conductor through the plasma. The current channel broadens quickly; after 36 ns the width of the current channel is about 4 cm. An effective resistivity can be calculated from this data using

$$\eta \approx \mu_0 \ell^2/t, \qquad (2)$$

where η is the resistivity in ohm-cm, $\mu_0 = 4\pi \times 10^{-11}$ H/cm, ℓ (cm) is the current channel width and t(s) is the penetration time. Using ℓ = 4 cm and t = 36 ns, $\eta \approx 5$ ohm-cm, which is three orders of magnitude larger than the transverse Spitzer resistivity[7] (for $T_e \sim$ 5eV). Buneman and ion-acoustic instabilities are possible causes of the enhanced collision frequency ($\sim 10^{10} s^{-1}$). The current channel width is much larger than the collisionless skin depth; c/ω_{pe} = 0.1 cm for $n_e = 3 \times 10^{13}$ cm^{-3} (measured with an electric probe[8]).

A theoretical model of the PEOS that accounts for the observed switching behavior has been developed.[9] In this theory, current is conducted in a bipolar, space-charge-limited fashion across a small gap at the cathode side of the PEOS. The maximum current that the PEOS can conduct (without opening)

is determined by the flux of ions to the cathode. The ion flux density is

$$\Gamma_i = n_i v_D, \tag{3}$$

where n_i is the ion density and v_D is the average ion drift velocity toward the cathode. The ratio of electron to ion current density across the gap (for the non-relativistic case) is

$$j_e/j_i = (M_i/Zm_e)^{1/2}, \tag{4}$$

where m_e (M_i) is the electron (ion) mass and Ze is the ion charge. The current through the plasma can increase until $j_i = \Gamma_i Ze$. A further increase in current causes the cathode gap to open, effectively increasing the ion current. This process is termed erosion of the plasma. During the erosion phase current begins to flow to the load. When the magnetic field in the gap is large enough to begin magnetic insulation of the cathode electrons, the ion current is larger than the value predicted by Eq. (4), similar to the enhancement that occurs in ion diodes.[10] This enhanced ion current causes the gap to open faster, accounting for the observed fast switching. With this large gap, the switch current is effectively cut off due to magnetic insulation of the electrons, leaving only a small ion current flowing across the gap.

The broadening of the current channel can be explained by this model, because the ion flux imposes a current density limit at the cathode during the conduction phase. If the current increases with a constant ion current density, $j_i = \Gamma_i Ze$, the current channel at the cathode will broaden. Using Eqs. (3) and (4), the electron current density limit is:

$$j_e < n_i v_D e (ZM_i/m_e)^{1/2} . \qquad (5)$$

The plasma ions are mostly C^{++},[8] so that $j_i/j_e \sim 0.01$, and the expression in Eq. (5) approximates the total current density, $j \sim j_e$. An equation for the current channel width, $\ell(t)$, is found using $I=2\pi r_c \ell j$, where r_c is the cathode radius and I is the total switch current. Solving for ℓ gives

$$\ell(t) = \frac{I(t)}{2\pi r_c n_i v_D e} \left(\frac{m_e}{ZM_i}\right)^{1/2} . \qquad (6)$$

For the Gamble I experiment, $Z \approx 2$, $n_i \approx 1.5 \times 10^{13}$ cm^{-3} and $v_D \approx 6 \times 10^6$ cm/s.[8] Eq. (6) then predicts $\ell \approx 1$ cm when $I \approx 37$kA, $\ell \approx 3$ cm when $I \approx 130$kA. This is consistent with the measured current channel width in the plasma [Figs. 4(a) and (b)]. Some deviation from this simple calculation is expected because of the known nonuniformity in $r_i(z)$ along the 6 cm switch length.[8] Enhanced plasma resistivity would allow the current channel width in the plasma to follow the width of the current channel at the cathode. This resistivity may be the result of instabilities caused by high velocity electrons from the cathode that stream past the plasma ions.

The current channel is accelerated in the z direction because of jxB forces during the 40 ns conduction period. The plasma boundary on the generator side of the PEOS is near $z \approx 0$ before the generator is fired. This boundary evidently moves 2 cm in the axial direction (Fig. 4) while the front of the current channel moves 6 cm (because of diffusion) in the same time period.

Figs. 4(c) and (d) show that the current is diverted to the load when the current path is disrupted near the inner conductor. This is attributed to the

increasing radial gap between the plasma and the cathode. The mechanism for gap formation is assumed to be erosion of the plasma and not magnetic pressure; magnetic forces in the radial direction are small between t = 36 ns and 46 ns (Fig. 4). After opening, a large fraction of the current continues to flow through the plasma. These plasma currents decay in about 100 ns (Fig. 3), a much longer time than the observed penetration time. This decrease in resistivity is consistent with magnetic insulation of the emitted cathode electrons which no longer drive instabilities in the plasma. The small gap size (<0.5 cm) indicated in Fig. 4(d) is due to the low impedance load used in these experiments; numerical modeling shows much larger gap formation when finite impedance loads (diodes) are employed.

The magnetic field measurements presented here give a picture of the current flow pattern in a PEOS. The current channel through the plasma broadens rapidly and becomes much larger than the skin depth, c/ω_{pe}. The inferred resistivity is anomalously large. The channel width is consistent with a current density limit determined by the ion flux to the cathode. Rapid switching occurs when a gap opens at the cathode side of the PEOS. Radial jxB forces are small at the time the gap opens, so erosion of the plasma is assumed to be the dominant opening mechanism. After opening, current continues to flow through the plasma but magnetic insulation prevents electron conduction across the gap.

The authors would like to acknowledge the technical assistance of P. Bell and discussions with Shyke A. Goldstein and R. Kulsrud. This work was supported by the Defense Nuclear Agency, the U. S. Department of Energy and the Office of Naval Research.

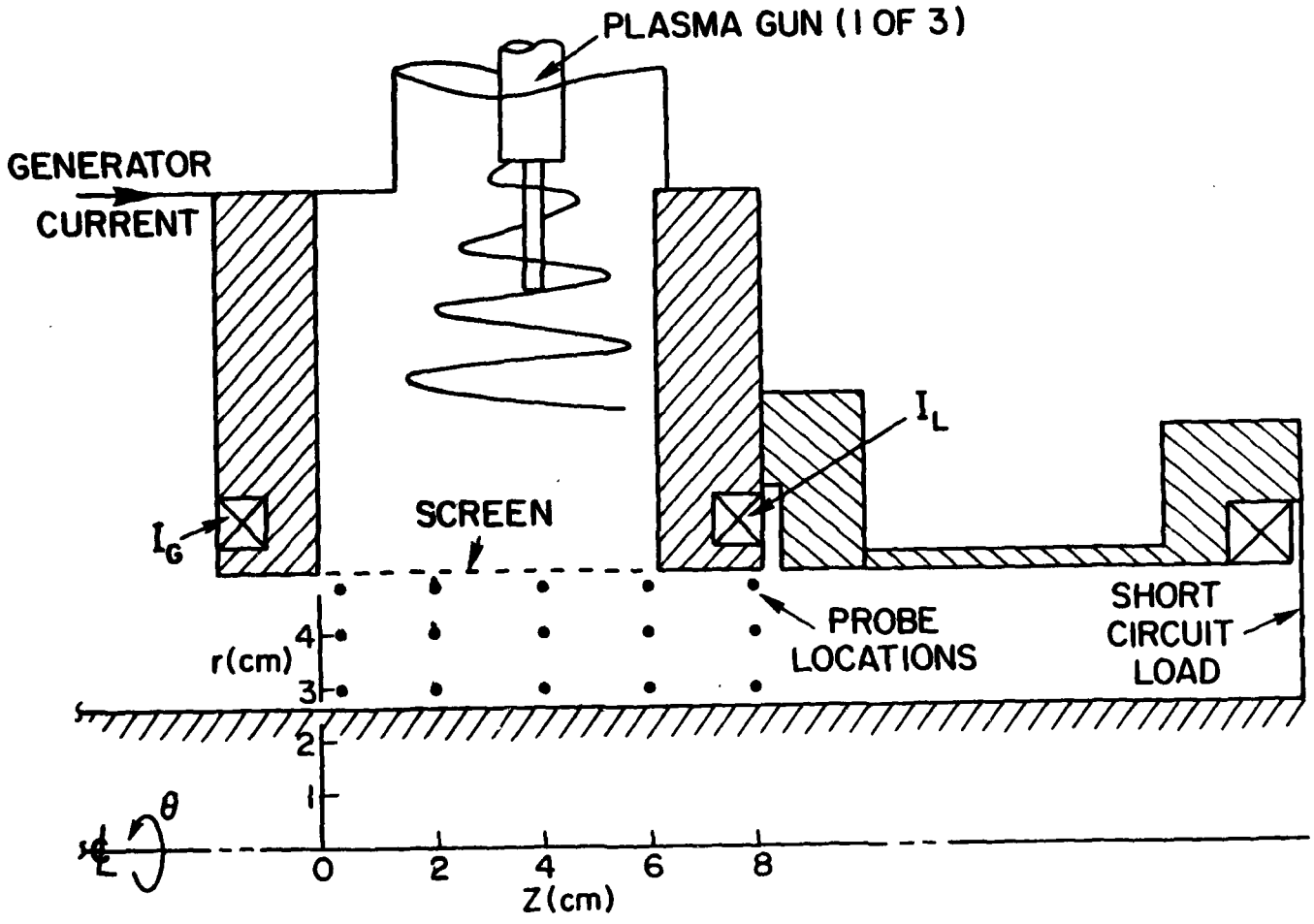

Fig. 1 — Gamble I PEOS Experiment: Rogowski loops measure the current on the generator side of the switch, I_G, and the load side of the switch, I_L. Dots indicate the data grid sampled to determine the current distribution.

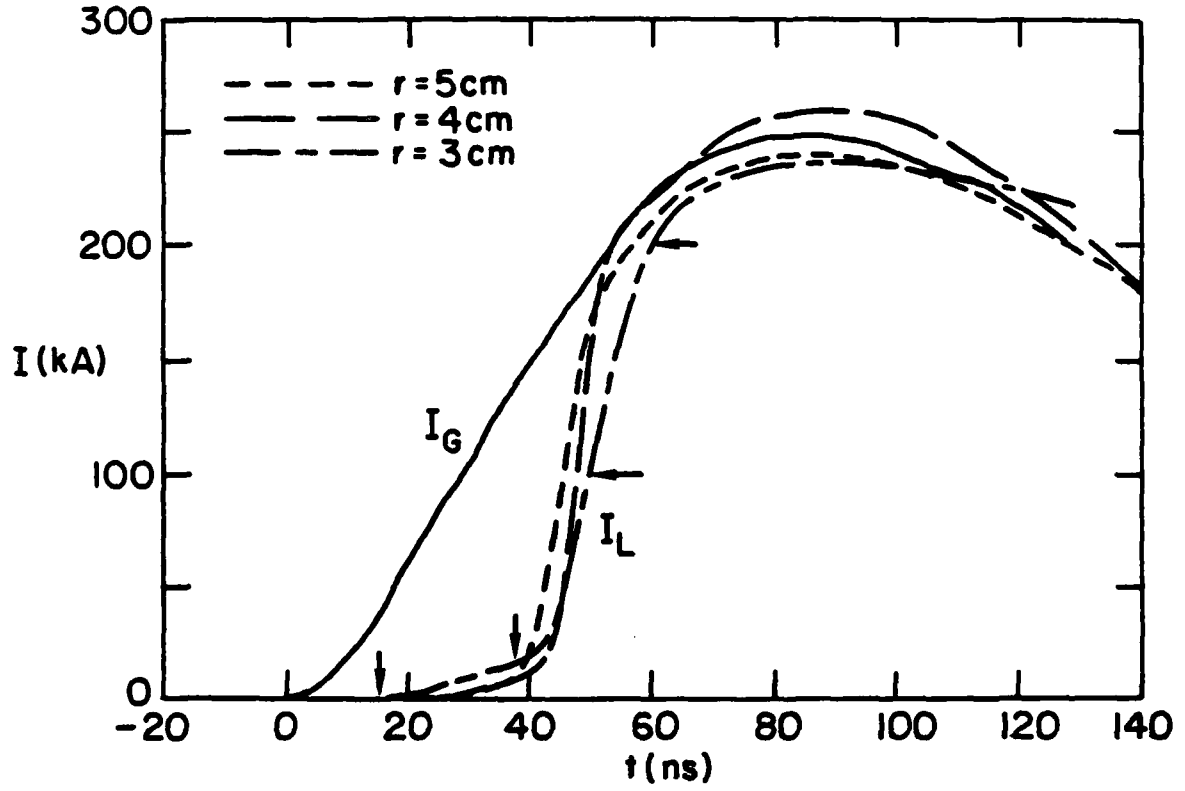

Fig. 2— Current Measurements: Three load currents (I_L) and one generator current (I_G) are shown, illustrating the fast opening property of the PEOS. The I_L measurements are for different radial locations of the probe array. The four I_L values marked in the figure are analyzed to determine the current distribution.

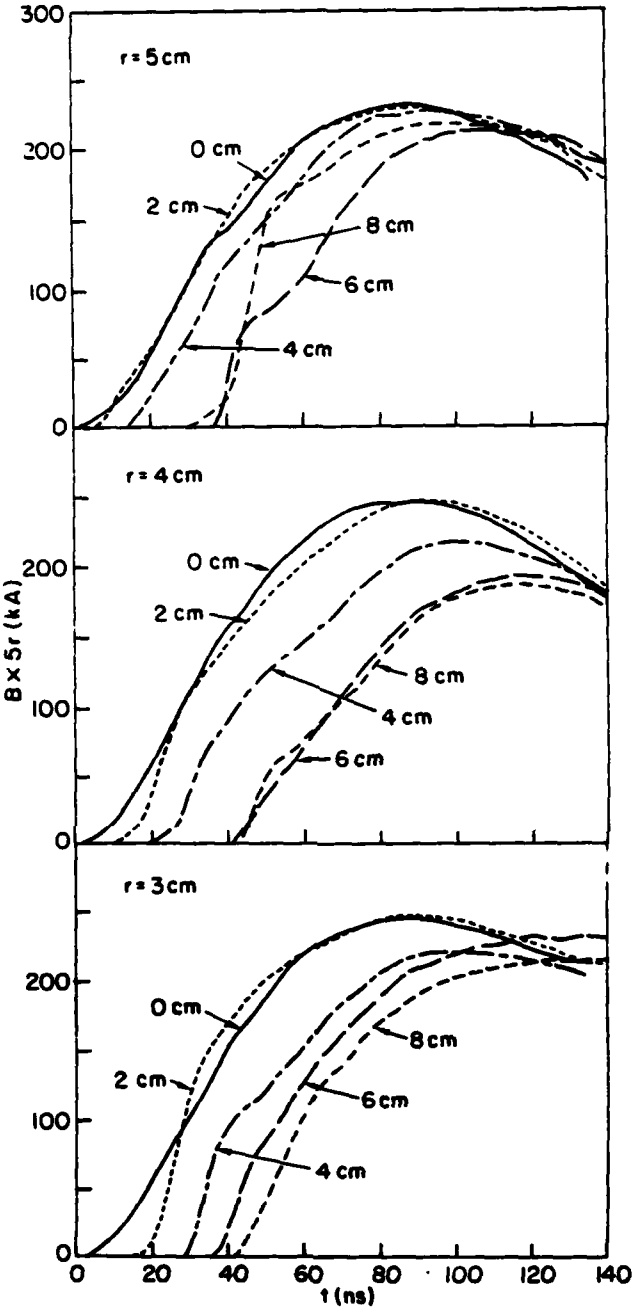

Fig. 3 — Field measurements are shown with the probe array at $r = 3$, 4, and 5 cm. The probe signals are normalized to the system currents using $I = B_\theta \times 5r$.

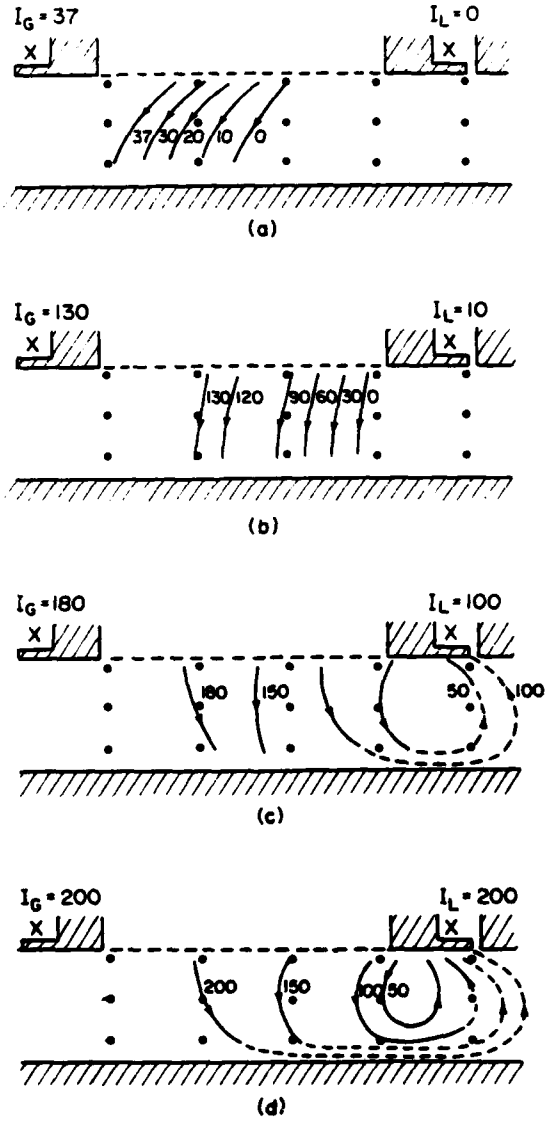

Fig. 4 — Current streamlines through the plasma are drawn (using the data in Figure 3), at the four times indicated in Figure 2. Each diagram shows the I_G and I_L values (in kA). (a) and (b): Current is conducted in the radial direction over a broad channel while the PEOS is "closed." (c) The current is diverted to the load near the downstream end of the switch region. (d) The current flows through the plasma within 0.5 cm of the inner conductor.

References:

1. R. A. Meger, R. J. Commisso, G. Cooperstein and Shyke A. Goldstein, App. Phys. Lett. 42, 943 (1983); C. Yamanaka, K. Imasaki, S. Miyamoto, T. Ozaki, S. Nakai, Y. Kato and T. Yabe, 1983 IEEE Int. Conf. on Plasma Science Abstracts (St. Louis, MO, May 1984), p. 82.

2. C. W. Mendel, Jr. and S. A. Goldstein, J. Appl. Phys. 48, (3) 1004 (1977); R. A. Meger and F. C. Young, J. Appl. Phys. 53, (12) 8543 (1982).

3. R. Stringfield, R. Schneider, R. D. Genuario, I. Roth, K. Childers, C. Stallings and D. Dakin, J. Appl. Phys. 52, (3) 1278 (1981).

4. J. P. VanDevender, Proc. 5th Int. Conf. on High Power Particle Beams (San Francisco, CA, Sept. 1983), p. 19.

5. G. Cooperstein, J. J. Condon and J. R. Boller, J. Vac. Sci. Technol. 10, 961 (1973).

6. C. W. Mendel, Jr., D. M. Zagar, G. S. Mills, S. Humphries, Jr. and S. A. Goldstein, Rev. Sci. Inst. 51, (12) 1641 (1980).

7. L. Spitzer, Physics of Fully Ionized Gases, 2nd rev. ed. Interscience, New York, 1962, p. 143.

8. J. M. Neri, R. J. Commisso, S. A. Goldstein, R. A. Meger, P. F. Ottinger, B. V. Weber and F. C. Young, 1983 IEEE Int. Conf. on Plasma Science Abstracts (San Diego, CA, May 1983), p.124.

9. P. F. Ottinger, S. A. Goldstein and R. A. Meger, J. Appl. Phys., 56 774 (1984).

10. S. A. Goldstein and R. Lee, Phys. Rev. Lett. 35, 1079 (1975).

DISTRIBUTION LIST

Director
Defense Nuclear Agency
Washington, DC 20305
Attn: TISI Archieves 1 copy
TITL Tech. Library 3 copies
J. Z. Farber (RAEV) 1 copy
C. Shubert (RAEV) 1 copy
J. Benson (RAEV) 1 copy

U.S. Department of Energy
Division of Inertial Fusion
Washington, DC 20545
Attn: L. E. Killion 1 copy
M. Sluyter 1 copy
R.L. Schriever 1 copy

U.S. Department of Energy
Office of Classification
Washington, DC 20545
Attn: Robert T. Duff 1 copy

U.S. Department of Energy
Nevada Operations Office
Post Office Box 14100
Las Vegas, NV 89114
Attn: Rex Purcell 2 copies

U.S. Department of Energy
P.O. Box 62
Oak Ridge, TN 37830 2 copy

Air Force Office of Scientific Research
Physics Directorate
Bolling AFB, DC 20332
Attn: H. Pugh 1 copy
R. J. Barker 1 copy

Air Force Weapons Laboratory, AFSC
Kirtland AFB, NM 87117
Attn: NTYP (W. L. Baker) 1 copy

Atomic Weapons Research Establishment
Building H36
Aldermaston, Reading RG 7 4PR
United Kingdom
Attn: J.C. Martin 1 copy

Boeing Company, The
P.O. Box 3707
Seattle, WA 98124
Attn: Aerospace Library 1 copy

Brookhaven National Laboratory
Upton, NY 11973
Attn: A.F. Maschke 1 copy

BMO/EN
Norton AFB, CA
Attn: ENSN 1 copy

Commander
Harry Diamond Laboratory
2800 Powder Mill Rd.
Adelphi, MD 20783
(CNWDI-INNER ENVELOPE: ATTN: DELHD-RBH)
Attn: DELHD-NP 1 copy
DELHD-RCC -J.A. Rosando 1 copy
DRXDO-RBH -J. Agee 1 copy
DRXDO-TI - Tech Lib. 1 copy

Cornell University
Ithaca, NY 14850
Attn: D.A. Hammer 1 copy
R.N. Sudan 1 copy

Defense Advanced Research Project Agency
1400 Wilson Blvd.
Arlington, VA 22209
Attn: R. L. Gullickson 1 copy

Defense Technical Information Center
Cameron Station
5010 Duke Street
Alexandria, VA 22314
Attn: T.C. 2 copies

JAYCOR, Inc.
205 S. Whiting Street
Alexandria, VA 22304
Attn: D. D. Hinshelwood 1 copy
P. F. Ottinger 1 copy
B. V. Weber 1 copy
J. M. Grossmann 1 copy

Kaman Tempo
816 State Street (P.O. Drawer QQ)
Santa Barbara, CA 93102
Attn: DASIAC 1 copy

KMS Fusion, Inc.
3941 Research Park Drive
P.O. Box 1567
Ann Arbor, MI 48106
Attn: Alexander A. Glass 1 copy

Lawrence Berkeley Laboratory
Berkeley, CA 94720
Attn: D. Keefe 1 copy

Lawrence Livermore National Laboratory
P.O. Box 808
Livermore, CA 94550
Attn:
Tech. Info. Dept. L-3 1 copy
D.J. Meeker 1 copy
R.E. Batzel/J. Kahn,L-1 1 copy
J.L. Emmett, L-488 1 copy
E. Storm, L-481 1 copy
W.F. Krupke, L-488 1 copy
J. Lindl, L-477 1 copy

Los Alamos National Laboratory
P.O. Box 1663
Los Alamos, NM 87545
Attn: M. Gillispie/Theo.Div. 1 copy
S.D. Rockwood,ICF Prog. Mgr.
DAD/IF M/S 527 6 copies

Massachusetts Institute of Technology
Cambridge, MA 02139
Attn: R.C. Davidson 1 copy
G. Bekefi 1 copy

Maxwell Laboratories, Inc.
9244 Balboa Avenue
San Diego, CA 92123
Attn: J. Pearlman 1 copy

Mission Research Corporation
1400 San Mateo Blvd. SE
Albuquerque, NM 87108
Attn: B.B. Godfrey 1 copy

National Science Foundation
Mail Stop 19
Washington, DC 20550
Attn: D. Berley 1 copy

Naval Research Laboratory
Addressee: Attn: Name/Code
Code 2628 -TID Distribution 20 copies
Code 1001 - T. Coffey 1 copy
Code 4000 - W. Ellis 1 copy
Code 4040 - J. Boris 1 copy
Code 4700 - S.L. Ossakow 26 copies
Code 4701 - I.V.Vitkovitsky 1 copy
Code 4704 - C. Kapetanakos 1 copy
Code 4720 - J. Davis 1 copy
Code 4730 - S. Bodner 1 copy
Code 4740 - W. Manheimer 1 copy
Code 4760 - B. Robson 1 copy
Code 4770 - G. Cooperstein 10 copies
Code 4770.1 - F. C. Young 1 copy
Code 4773 - R.A. Meger 1 copy
Code 4773 - S.J. Stephanakis 1 copy
Code 4790 - D. Colombant 1 copy
Code 4790 - I. Haber 1 copy
Code 4790 - M. Lampe 1 copy
Code 6682 - D. Nagel 1 copy

Physics International Co.
2700 Merced Street
San Leandro, CA 94577
Attn: A.J. Toepfer 1 copy

Pulse Sciences, Inc.
1615 Broadway, Suite 610
Oakland, CA 94612
Attn: S. Putnam 1 copy

R&D Associates
Suite 500
1401 Wilson Blvd.
Arlington, VA 22209
Attn: P.J. Turchi 1 copy

SAI
8400 W. Park Ave.
McLean, VA 22102
Attn: A. Drobot 1 copy

R&D Associates
P.O. Box 9695
Marina Del Rey, CA 90291
Attn: C. MacDonald 1 copy

Sandia National Laboratories
P.O. Box 5800
Albuquerque, NM 87185
Attn: P.Vandevender/1200 6 copies

Spire Corporation
P.O. Box D
Bedford, MA 01730
Attn: R.G. Little 1 copy

Stanford University
SLAC
P.O. Box 4349
Stanford, CA 94305
Attn: W.B. Herrmannsfeldt 1 copy

University of California
Irvine, CA 92717
Attn: N. Rostoker 1 copy

University of Rochester
250 East River Road
Rochester, NY 14623
Attn: J. Eastman 1 copy

Univ. of Washington
Dept. of Nuclear Engineering
BF-10
Seattle, WA 98115
Attn: F. Ribe 1 copy

Director of Research
U.S. Naval Academy
Annapolis, MD 21402 2 copies

END

FILMED

4-85

DTIC